

Unconstrained motions, dynamic heterogeneities, and relaxation in disordered solids

Vanessa K. de Souza and Peter Harrowell

School of Chemistry, University of Sydney, Sydney, New South Wales 2006, Australia

(Received 15 May 2009; published 14 October 2009)

A disordered network of bonds with a fixed configuration can relax via a variety of unconstrained motions. These motions can be directly inferred from the topological arrangement of constraints without any geometrical information. We use the pebble game algorithm of Jacobs and Thorpe [D. J. Jacobs and M. F. Thorpe, *Phys. Rev. Lett.* **75**, 4051 (1995)] to decompose the system into separate rigid clusters and identify the remaining degrees of freedom. Unconstrained motions can then be resolved in the form of translations and rotations of isolated groups of bonds and the internal motion within bond groups. We show that each motion can be assigned a characteristic thermal velocity and hence a relaxation time scale. We use this information to construct a relaxation function and also examine the spatial distribution of relaxation time scales. We investigate the sensitivity of the relaxation time scales and their spatial distribution when making individual bond changes in the system, and we consider the dependence of these time scales on the underlying structure.

DOI: [10.1103/PhysRevE.80.041503](https://doi.org/10.1103/PhysRevE.80.041503)

PACS number(s): 64.70.qj, 63.50.Lm, 61.43.Fs

I. INTRODUCTION

Disordered solids typically exhibit an excess of low-frequency modes over that observed in the crystalline state of the same material [1,2]. These excess modes are quasilocal in character and arise directly from the failure of local particle arrangements to provide a homogeneous constraint of particle motion. The failure of liquid configurations to fully constrain the motion of the particles involved has long been acknowledged, although loosely expressed, in the concept of “free” volume. Recently [3], it has been demonstrated that the spatial heterogeneity of relaxation in a supercooled liquid is strongly correlated with the spatial heterogeneity of the low-frequency quasilocalized modes of the local potential minima. Soft normal modes, in other words, play exactly the role envisioned for free volume but with the advantage of being uniquely defined. Motivated by this result, we are interested in understanding the features of a disordered structure that determine the spatial heterogeneity of these soft modes, the degree of nonlocality involved in the structure-dynamics relationship and the factors that influence the evolution of the spatial distribution of soft modes. In this paper we describe an analysis of the spatial distribution of unconstrained motions in a disordered solid modeled using a random bond network.

Goldstein [4] suggested that the relaxation of deeply supercooled liquids is dominated by the potential energy surface. The local minima of the potential energy, christened “inherent structures” by Stillinger and Weber [5], correspond to zero-temperature disordered solids. From this energy landscape perspective [6–9], the dynamics of the deeply supercooled liquid is regarded as a temporal sequence of disordered solids, linked by localized reorganization events. The glass transition is essentially the temperature at which a particular disordered solid, or connected group of such solids, persists for the time scale of the observation. The connection between the relaxation of the supercooled liquid and the quasilocalized soft modes is that these modes appear to be the collective motions by which the irreversible transition between inherent structures is accomplished [3]. Brito and

Wyart [10] showed that, in liquids simulated using small systems, the intermittent relaxation events project almost completely onto a single soft normal mode. Establishing a direct and intuitive connection between soft modes and the structures that give rise to them is the goal of this work. Understanding how a configuration determines the spatial pattern of motions is of central importance in developing a useful microscopic treatment of glass transitions.

We need a simple and general description of disordered solids with which to model the inherent structures. This description must allow us to identify the soft modes, their spatial distribution, and their relationship to the configurations with which they are associated. A representation of the disordered solids by constraint networks meets these requirements. Focusing on the topology of constraints, Phillips [11] and Thorpe [12] developed a powerful treatment of the global character of rigidity in network glasses. In a network of rigid rotating bonds (“bars”) a cluster of sites connected by bonds can belong to a single rigid cluster, with no internal degrees of freedom remaining unconstrained. The only possible motions remaining to the particles in such a rigid cluster involve the rotation and translation of the cluster as a whole (distortions of the bonds, and hence vibrations, having been excluded by construction). The criterion for the rigidity of a cluster of N particles in d dimensions is that the total number of internal degrees of freedom, i.e., $dN - d(d+1)/2$, equals the number of nonredundant bonds. Maxwell [13], in first treating this problem, applied the condition by counting the number of bonds. This simple counting of constraints neglects the possibility that some of the bonds have been placed between particles that were already fully constrained and, therefore, these bonds represent overconstraints. In 1995, Jacobs and Thorpe [14,15] developed an algorithm to enumerate these overconstraints (in two dimensions) and so determine, explicitly, the remaining floppy modes (i.e., unconstrained degrees of freedom) for a given realization of the constraint network. In this paper we shall demonstrate how this enumeration of floppy modes provides an explicit description of dynamic heterogeneities in the disordered network.

At this point, it is worth clarifying the definition of a solid in the context of constraints. A solid is a material that exhibits a nonzero yield stress under shear. This is first achieved, with increasing bond density, when rigid clusters first span the system. We shall, therefore, identify the onset of solidity with the rigidity percolation transition. The term *total rigidity*, in contrast, is used to describe a system in which no internal floppy modes exist. The transition to total rigidity will clearly occur at a density of bonds greater than that of the transition to solidity (rigidity percolation). For reference, in granular systems governed only by repulsive interactions, there is no rigidity percolation and what we call the total rigidity transition is referred to, equivalently, as the isostatic point or the jamming transition [16]. The basic thesis of this paper is that inherent structures of a supercooled liquid (a) are solids and (b) retain sufficient floppy modes to allow them to undergo transitions to other inherent structures. In the language of constraint networks, this thesis corresponds to the proposal that inherent structures are described by constraint networks lying between the appropriate solidity and total rigidity transitions.

To what amorphous solids do we think this type of model applies? The conceptual connection between the inherent structures of a covalent network-forming liquid such as silica and a random network of bonds (with an appropriate coordination number) is straightforward. Although less obvious, important connections also exist between constraint networks and close-packed glasses (such as amorphous metallic alloys), certainly at least to the degree that such glasses resemble granular packings. Constraint theory has been applied to problems of granular packing [17] since 1990. One difficulty for the application of constraint counting to close-packed glasses is that there appears to be just too many neighbors. In random close-packed hard spheres, for example, the average number of neighbors is ~ 8 , where neighbors are defined as particles within 1.057 of a diameter of each other [18]. If each neighbor represented a constraint, then close-packed arrays of spheres such as this would correspond to a significantly overconstrained system and, hence, one for which the balance between the number of constraints and degrees of freedom would appear to be of little relevance. The fallacy of this view was demonstrated by Moukarzel [19] who pointed out that steric packings (i.e., packings of particles interacting by short-range repulsions) cannot typically sustain such an overconstraint and that the number of actual constraints (i.e., contacts) is considerably less than the number of nearest neighbors (as defined above). As a result, rigidity corresponds to the isostatic condition, i.e., an exact balance of constraints and internal degrees of freedom. The theoretical argument [19] has been supported by the numerical results of Donev *et al.* [20]. Constraint counting, in other words, remains of central importance to the question of rigidity across a broad range of disordered solids. While acknowledging that there are unresolved questions concerning the relationship between floppy modes of the bond network and those of a dense amorphous arrangement of particles dominated by steric interactions [19,21], we present our results with the belief that the local fluctuations in constraint in the bond networks, analyzed in this paper, provides useful insights into the relationship between

structure and dynamic heterogeneity in amorphous materials in general, not just the covalent glasses.

The connection between fluctuations in constraints and soft modes has already been explored in the study of protein dynamics and of excess low-frequency modes in jammed granular material. Jacobs *et al.* [22] pointed out that substantial increases in efficiency for simulations of large amplitude motions in globular proteins can be achieved if only the equations of motion for the degrees of freedom associated with soft modes are integrated. Employing an algorithm similar in spirit to that described in this paper, these authors have implemented this approach in a set of public domain routines [23]. The influence on jamming transitions resulting from the existence of soft local modes has also been studied [24]. Wyart *et al.* [25,26] developed a comprehensive picture of the dispersion of soft modes as the jamming transition is approached from the high density side. Driven granular material has been found to exhibit dynamic heterogeneities similar to those seen in glass-forming liquids [27–29].

In a previous brief report [30], we have outlined some results obtained from an analysis of unconstrained motions in a network of constraints over a range of bond densities. In this paper, we describe in detail the methods used to define and characterize these motions. In the following section (Sec. II) we introduce the pebble game algorithm and summarize the treatment of constraints and floppy modes introduced by Phillips and Thorpe to the study of network glass-forming liquids. In Sec. III, we introduce the concept of unconstrained motion. Our focus is on obtaining a characterization that is unambiguous and we discuss two different methods for defining unconstrained motions. In Sec. IV we explain the methods used to obtain a spatial distribution of these unconstrained motions on a triangular lattice. We can obtain a relaxation function for the random network as described in Sec. V, where we also examine changes in relaxation time scales and their distribution when bonds are moved.

II. CONSTRAINT COUNTING

A. Model

Our goal here is to address the general problem of motion in a network of constraints—how to define the soft modes and to characterize their relaxation properties and spatial distribution. As our subsequent description of particles involves only the topology of constraints between them, the geometrical features of the lattice are irrelevant. Constraints, in the form of rigid bonds between neighboring particles, are assigned at random within the confines of a two-dimensional (2D) triangular lattice. Particles are represented by vertices of the lattice in periodic boundary conditions. Each set of connected vertices represents an inherent structure of the 2D liquid. The results shown herein have been obtained using a 2500 site lattice, but we have studied system sizes varying from 100 to 10 000 vertices.

B. Redundant bonds and floppy modes

In 1979, Phillips used the stability condition, developed by Maxwell to describe trestle structures, to address the ri-

rigidity of network glasses [11]. Each point in d dimensions has d degrees of freedom. A rigid cluster, formed by a collection of points, has $d(d+1)/2$ degrees of freedom. Therefore, to form a rigid cluster, there must be at least $dn-d(d+1)/2$ connections (or constraints) between the n points. In granular studies [17,31], the form of the constraints between particles are not the same as those found in the linear elastic networks of network glasses. Forces between the particles are compressive only and these constraints are known as *struts*. Another form of constraint is a *cable*, which can only sustain tensile forces. Networks with either of these constraints are *sign constrained*. Combining elements of both types can lead to interesting properties forming a *tensegrity* structure [32,33]. In this paper, we shall consider only rigid bonds (known as bars) between pairs of particles. There are both compressive and tensile forces between particles, representing a long-range attraction and a short-range repulsion.

If a rigid cluster of n points has exactly $dn-d(d+1)/2$ bars, it *could* be minimally rigid or isostatic. However, to determine the number of degrees of freedom remaining in the system (the floppy modes), we cannot simply count the number of bars. A bar can be redundant—that is, the bond has been placed between two particles that are fully constrained already, with the result that there is a local overconstraint. To count the true number of floppy modes in a network, it is necessary to identify these redundant constraints. This problem was solved in two dimensions by Jacobs and Thorpe [14,15] with their introduction of the pebble game algorithm. The algorithm calculates the number of floppy modes, locates regions that are overconstrained, and decomposes the system into separate rigid clusters.

The pebble game represents degrees of freedom as movable objects, known as “pebbles.” For a system in two dimensions, the degrees of freedom available to a particle or lattice site are represented initially by two pebbles attached to each site (in d dimensions there would be d pebbles per site). The algorithm moves pebbles from their original sites and onto bonds such that pebbles are only moved to bonds connected to their original site, there is no more than one pebble per bond, and the number of pebbles moved onto bonds is maximized. The pebbles on bonds correspond to the degrees of freedom removed by the bond constraints. Bonds are added to the system one at a time and, for each new bond, pebbles are moved around the system, with the intention of obtaining two free pebbles on each of the newly connected sites, four in total. However, the movement of the pebbles is restricted by the conditions that all independent bonds must remain covered and that pebbles must remain attached to their original sites. It is always possible to collect three pebbles, but a fourth pebble corresponds to a floppy degree of freedom and one of the four collected pebbles can then be used to cover the bond. If four free pebbles cannot be found, the bond is redundant and an overconstrained region is identified. The overconstrained region consists of the set of bonds searched in trying to free the fourth pebble.

The completed network can be decomposed into separate rigid clusters, which define the structure of the system. A rigid cluster has only three degrees of freedom and no other floppy modes. Within the algorithm, rigid clusters are identified by testing pairs of sites. Two sites belong to the same

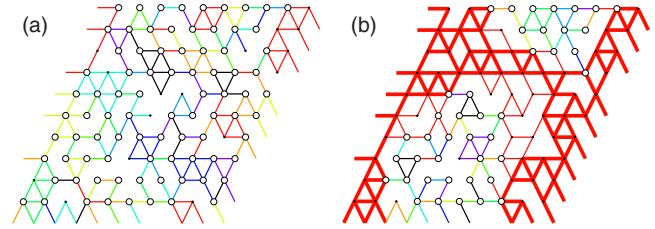


FIG. 1. (Color online) Two example systems based on a triangular lattice arrangement of 100 sites in periodic boundary conditions are shown. The left panel shows a system at a bond density of 0.633 (before the percolation transition) and the right panel shows a bond density of 0.667 (after the percolation transition). Lattice sites or vertices are shown either as open circles, for a pivot point, or as black dots. The lines show bonds between the vertices. The different shades indicate the presence of separate rigid clusters. Overconstrained regions, indicated by heavy lines, are present in the system on the right.

rigid cluster if an additional bond between them would be redundant. The degrees of freedom remaining in the system, *floppy modes*, are represented by pebbles which do not cover bonds but remain attached to their original sites. As well as rigid clusters, the system can also contain unbound particles, which retain their original two degrees of freedom.

For a triangular lattice with randomly placed bonds, the rigidity percolation transition, when the probability of finding a spanning rigid cluster undergoes an abrupt jump in magnitude, occurs at a bond density of 0.66 [14]. Figure 1 depicts a triangular lattice of 100 sites at bond densities before and after the percolation transition. Lattice sites are shown by black dots or open circles (these sites are pivots; see Sec. III) and lines show connecting bonds. The different shades indicate the presence of separate rigid clusters. The right panel shows a system containing overconstrained regions, which are indicated by heavy lines.

As the inherent structures we are looking to model are rigid structures, the relevant constraint networks are those above the rigidity percolation transition, with a bond density greater than or equal to 0.66. Our discussion shall be about the dynamic consequences of inherent structures being either at the rigidity percolation transition or at higher bond densities. We shall, however, include data from bond densities below the transition density for completeness.

In granular studies, local stability is associated with configurations at their isostatic state. Recent work by Wyart *et al.*, which includes a description of the origin of excess low-frequency vibrational modes [25,26], also describes systems that form an isostatic state and, in addition, have minimal fluctuations in coordination. In this paper, bonds are placed randomly in the triangular lattice, without regard for the nature of the bond. As we are not avoiding redundant bonds, we do not produce an isostatic state and there are large fluctuations in coordination. Even when redundant bonds are disallowed, the solidity onset (rigidity percolation) and the isostatic point do not necessarily coincide, with the former occurring at a slightly lower bond density than the latter [34]. We shall leave for future work the study of the influence of nonrandom bond distributions, such as those responsible for the isostatic state, on the heterogeneity of soft modes.

Weighting in favor of overconstraint is also possible, with the weighting arising from the stabilization of locally preferred structures with a high symmetry (which thus avoid the stress usually associated with overconstraint). It is possible that strong and fragile fluids might be distinguished by inherent structures that tend to the isostatic or overconstrained landscapes, respectively.

It is worth emphasizing that we are, with the constraint networks, modeling inherent structures and not the instantaneous structures we would expect to sample in a trajectory. The density of bonds or constraints is not a control parameter of the same form as temperature when cooling a supercooled liquid toward the glass transition. In this sense, the onset of solidity and total rigidity with changing bond density represents bounds within which we expect to locate the inherent structures rather than transitions observable by adjusting some experimental parameters. The transition from liquid to glass on cooling is the result of the rapidly growing residence times of the system in particular inherent structures and does not require any dramatic change in the nature of the inherent structures themselves.

III. UNCONSTRAINED MOTIONS

The pebble game contains a spatial distribution of floppy modes represented by the remaining free pebbles, and we would like to convert this representation into a spatial distribution of particle movement. Our answer to this problem is presented in three parts. First, we explain how to identify a set of particles associated with each free pebble, representing an unconstrained degree of freedom or floppy mode. Next, we demonstrate that this procedure must inevitably result in a spatial distribution with an element of arbitrariness. The situation is analogous to the arbitrary character of the eigenvectors of degenerate normal modes. Finally, we demonstrate an alternative method to identify, for each particle, the unconstrained motion to which they belong that involves the smallest number of particles. The number of these unconstrained motions exceeds that of the number of floppy modes and, thus, they cannot be independent of one another. Their great advantage, however, is that their spatial extent is free of the arbitrary aspects of the floppy modes.

Our first task then is to determine the sites over which a given floppy mode is distributed. To begin, we remind the reader that a pebble can only sit on the site to which it was assigned or on a bond directly connected to that site, so an individual pebble cannot move very far. It is possible, however, for an exchange “move” in which an initially free pebble is moved from its site to an adjacent bond while the pebble on that bond is moved to the site at the other end of the bond (see Fig. 2, right panel). The result is a free pebble disappears from one site and a free pebble appears at the site on the other end of the connecting bond. Via this process we can conclude that the two sites are part of the same floppy motion. Further sites are added to the collective mode by similar shuffling (not involving any other free pebbles initially present) until all possible permutations have been exhausted, leaving us with the final representation of the floppy mode. The procedure is then repeated for each of the free pebbles in turn.

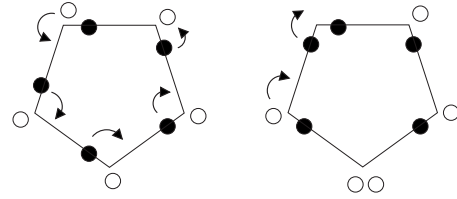


FIG. 2. The two panels show a system of five sites and five bonds forming a pentagon. Two possible arrangements of pebbles describing the degrees of freedom within the system are shown. The left panel shows a symmetrical pebble arrangement and the right panel shows one possible final arrangement resulting from a pebble game analysis of the system. In the symmetrical arrangement of pebbles, moving any of the free pebbles onto a bond and subsequent shuffling of pebbles to different bonds (ignoring any other free pebbles) allows a pebble to be freed at any of the other vertices of the pentagon; every degree of freedom is delocalized across the whole system. In the right panel, three of the free pebbles remain localized and cannot be moved around the whole system.

As indicated at the start of this section, there is a problem associated with asking for the spatial distribution of each floppy mode. The problem is that, if you renumber the sites so that the pebble game carries out its moves in a different sequence, you can get a different spatial picture of the floppy modes. While the differences are often slight, they are disconcerting and obviously call to question the physical significance of the spatial pictures of the modes. For an example, we show a pentagonal cluster in Fig. 2. Two different distributions of the five free pebbles are depicted, representing two internal modes. While the symmetric distribution (left panel) results in the overall modes and both internal modes involving all five particles, for the asymmetric distribution (right panel), the overall rotation is not easily separated out and we are left with three internal modes: two involving two particles and one involving three particles. The sequential nature of the pebble movements in the pebble game means that the final deposition of free pebbles depends on the sequence in which the moves were performed.

This problem with using a direct floppy mode analysis is resolvable, for example, with appropriate rules where one could define a set of floppy modes with a minimal spatial extent. However, it is worth reflecting on the information that we require with regard to the spatial distribution of modes. We are interested in how mobility is related to structure and therefore require an intuitive connection between the structure and the resulting dynamics. In molecular dynamics simulations, dynamic heterogeneities are defined in terms of some measure of mobility assigned to each particle. In the context of the constraint network, we can ask an analogous question. For each particle, what is the unconstrained motion to which they belong that involves the smallest number of particles? We chose the smallest one because that will be the fastest mode of relaxation available to that particle. The problem of describing the spatial extent of floppy modes has previously been addressed for the analysis of flexibility in proteins [22,23,35,36]. The biomolecular flexibility analysis software (FIRST) [23] includes a calculation of a “flexibility index,” which sidesteps the issue by calculating a density of

floppy modes rather than considering each mode individually, and a method involving the locking of rotatable bond dihedral angles (or pivots) has also been implemented [22,37]. Here, we shall introduce a similar method for a two-dimensional system which includes the concept of a pivot cluster—a set of rigid clusters connected by flexible linkages.

This alternative description of motion within the system can be obtained by using information from the pebble game in terms of the different rigid clusters in the system and the sites connecting these different rigid clusters that are called *pivots*. Unconstrained motions in the constraint network for isolated collections of bonded sites come in two forms. Each isolated (or free) cluster has three unconstrained degrees of freedom (two translational and one rotational). The second type of unconstrained motion arises from flexions within nonrigid free clusters. A nonrigid cluster can be resolved into a set of rigid subclusters linked together by common sites that act as pivots. A single free cluster may include many pivots. In fact, there are normally many more pivots within the system than remaining degrees of freedom (i.e., unassigned pebbles), as the motion of each pivot is not normally independent of the other pivots in the system.

We identify unconstrained motions using the following protocol: (1) all isolated sites have two degrees attached to them (translational modes); (2) all isolated clusters have three degrees of freedom distributed evenly across all the participating vertices (translational and rotational modes, these clusters can be composed of groups of rigid clusters that are connected by pivots); and (3) for each pivot point (i.e., a vertex common to two or more different rigid clusters) a bond is placed across the pivot so that the two adjoining clusters are linked. The pebble game routine is rerun and the change in rigid clusters due to the probe bond is determined. In this way, by placing a bond across each pivot and noting the other pivots which no longer exist as a result of placing this bond, groups of pivots can be identified. The clusters joined together by pivots within the same group form a *pivot cluster*. Each pivot cluster describes one unconstrained motion.

If the pivot grouping described above is done by testing each pivot separately, the result is found to be independent of the starting positions of the free pebbles and the order of pivot testing, and so provides a unique description of movement within the system that does not depend on the order of bond construction. This is demonstrated in Fig. 3, where we compare the floppy mode (right panel) and the unconstrained motion (left panel) methods for the interconnected lattice structure shown in the left panel of Fig. 1. Four different lattice site labeling schemes are used so that bonds are added to the system in a different order; the resulting movement of pebbles changes as well as the order of pivot testing. Results are identical for the unconstrained motion analysis; but, for the floppy mode analysis, different site labels result in different distributions of modes.

For the unconstrained motion analysis, we typically find more unconstrained motions than there are floppy modes, so that while the floppy modes are independent, the unconstrained motions generally are not. Again we can illustrate this feature with the pentagonal cluster (see Fig. 4). With

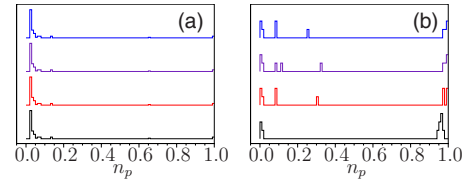


FIG. 3. (Color online) Distributions of participation ratios n_p , for all motions in the system, are shown for the interconnected lattice structure in the left panel of Fig. 1. The results are derived from an analysis of unconstrained motions (left panel) and an analysis of floppy modes (right panel). The graphs compare results for four different site labeling schemes and the histograms have been shifted vertically for clarity. The results are identical in the unconstrained motion analysis, confirming that the representation of unconstrained motions is unique. The same cannot be said for the representation of modes from the floppy mode analysis as we see that different site labels result in different distributions of modes.

only two internal floppy modes, the pentagon has five pivot points and so five unconstrained motions. Due to the presence of the ring, movements about pivot points are not independent. Figure 5 shows the average ratio of possible unconstrained motions to the number of floppy modes for a range of bond densities. The unconstrained motions include three modes (translation and rotation) for each free cluster, two modes (translation) for each free particle, and one mode for each pivot cluster. If our identification of unconstrained motions required that they are independent, then there could only be as many unconstrained motions as there were floppy modes and the ratio in Fig. 5 would be 1. The ratio peaks before the percolation transition at a bond density of ~ 0.65 . The high value at this bond density can be attributed to the presence of ring structures formed by rigid clusters and connecting pivots. Statistics for the number of unconstrained motions and as well as their distributions as functions of bond density can be found in Ref. [30].

To summarize, the unconstrained motions in a constraint network are the combination of the movement of isolated free clusters and the internal flexing of rigid clusters joined by pivots. In the next section, we shall explain how to translate the size of a cluster, free or pivot, into a time scale for the unconstrained motion of the particles belonging to that cluster.

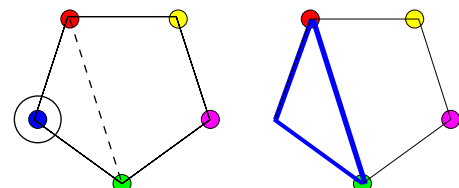


FIG. 4. (Color online) For a system of five sites joined together to form a pentagon, a pebble game analysis shows that each bond is a separate rigid cluster. Therefore, pivot points connecting different rigid clusters are present at each vertex. The left panel shows a test bond, represented by a dashed line, placed across the leftmost pivot. The right panel shows the resulting rigid cluster of three bonds formed by this test bond. None of the other bonds are affected by this new bond and there are four remaining pivots.

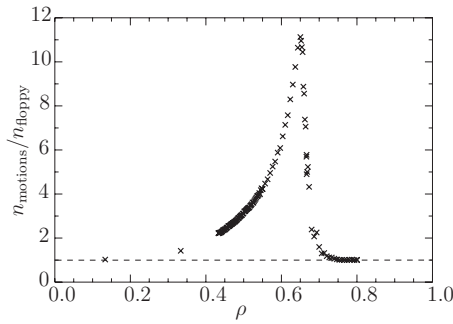


FIG. 5. The average number of unconstrained motions per floppy mode, $n_{\text{motions}}/n_{\text{floppy}}$, is shown as a function of bond density ρ . The unconstrained motions include three modes—two translations and one rotation—for each free cluster, two modes (translation) for each free particle, and one mode for each group of interdependent pivots. The dashed line shows the ideal ratio of one unconstrained motion per floppy mode.

IV. ASSIGNING TIME SCALES

For each unconstrained motion, there is a characteristic thermal velocity determined by the inertia and the temperature. If a particular motion involves a large number of particles, the associated thermal velocity will be slower. The process of calculating a time scale is simple for the relaxational modes of the free clusters. For the one rotational mode, we can obtain the equilibrium average of the angular velocity from the moment of inertia I of the whole cluster as follows:

$$\langle \Omega^2 \rangle = \frac{k_B T}{I}. \quad (1)$$

The role of the temperature here is simply to rescale all angular velocities so, in the following discussion, we shall set $k_B T = 1$. The moment of inertia is calculated by assigning a mass of 1 to each lattice site and a length of 1 unit to the distance between adjacent sites. The total mass of the cluster, therefore, is given by the number of constituent sites, and this replaces the moment of inertia to give the characteristic velocity of the two translational modes.

Structural relaxation requires that a particle's position becomes decorrelated with its position, and those of its neighbors, at an earlier time. Particles confined within a free cluster can still undergo such a relaxation via this translation and rotation of the cluster as a whole. We shall therefore identify the inverse thermal velocity of the cluster as the structural relaxation time τ for that cluster, so that

$$\tau = \langle \Omega^2 \rangle^{-1/2}. \quad (2)$$

We must also assign time scales to the internal motions within free clusters, which we have resolved into groups of rigid clusters connected by interdependent pivots, or pivot clusters. The motion within a pivot cluster can be likened to a model studied by Zwanzig, consisting of random clusters of intermeshed cogs [38]. In the Zwanzig model, the moment of inertia is equal to the sum of the individual moments of inertia of all the coupled cogs in the cluster; the rotation of any one cog requires the rotation of all the other cogs in the

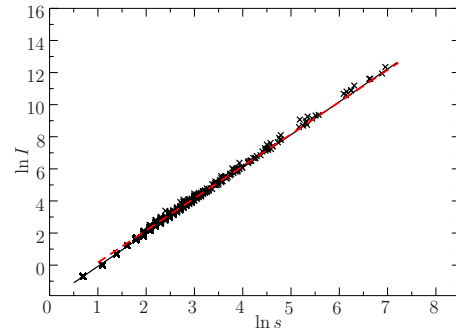


FIG. 6. (Color online) The variation in the moment of inertia I of rigid clusters with their size s . Cluster size is given by the number of bonded sites in the cluster. The data are taken from systems with bond densities between 0.433 and 0.67. The solid line shows a linear regression fit to the data, $y = -2.13 + 2.05x$. The dashed line is the relationship expected for solid disks with a uniform mass.

cluster to which the one of interest belonged. The comparison is imprecise as we need to restrict the cogs to small angular motions; but with this restriction, they provide a simple picture of the motion of the rigid clusters that make up a pivot cluster, with pivots acting as the cogs' meshed teeth. The rotation of any rigid cluster in the pivot group requires the motion of other rigid clusters in the group. Hence, the moment of inertia of the pivot cluster is related to the sum of the moments of inertia of all the rigid clusters which make up that pivot cluster. Our first step therefore is to determine the moments of inertia of each individual rigid cluster.

Figure 6 shows moments of inertia for rigid clusters of varying size. These clusters were found for random bond arrangements within the triangular lattice of 2500 sites with bond densities between 0.433 and 0.67. A linear regression fit to the data provides a good representation of the relationship between cluster size and moment of inertia, $\ln I = -2.13 + 2.05 \ln s$. Despite the variety of shapes of the rigid clusters, we find that the relation between I and s for the clusters is very similar to that of solid disks with a uniform mass. Therefore, it appears to be unnecessary to calculate the moment of inertia for each rigid cluster. Instead, we can use the size of the cluster to estimate its moment of inertia. (The same method can also be applied to calculating the moment of inertia of free clusters.) The compact nature of the clusters is surprising; this would not be expected for studies of connectivity rather than rigidity percolation.

As we will later be concerned with finding the fastest motions for each site, our scheme for determining the total moment of inertia and hence the relaxation time scale of a pivot cluster requires a small modification. Consider an isolated cluster consisting of two rigid clusters, one large and one small, linked at a pivot point as shown in the two panels of Fig. 7. Using our current method, the sum of the moments of inertia will be dominated by the larger rigid cluster. This obscures the fact that the smaller cluster can move, relative to the position of its larger partner in a manner that is independent of the size of the large cluster (left panel). The relevant moment of inertia for this relaxation is merely that of the smaller cluster itself. To assign a time scale to the larger

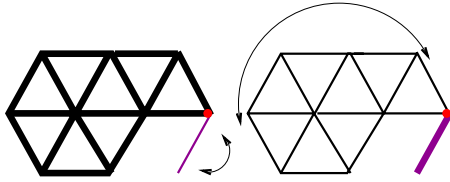


FIG. 7. (Color online) The two panels show a pivot cluster formed from one large rigid cluster and one small rigid cluster, which is a single bond. Motion of the small cluster is independent of the size of the large cluster as indicated in the left panel. By the same token, we can describe the motion of the larger rigid cluster with the small cluster frozen in position (right panel).

cluster, we can consider its movement relative to the smaller cluster fixed in position (right panel), and again the relevant moment of inertia is that of the single cluster.

This method can be extended to pivot clusters comprised of more than two rigid clusters. In effect, for each pivot cluster, we are calculating the two shortest possible time scales for relaxation. The first time scale is obtained by fixing the largest rigid cluster, and this time scale is applied to the particles in all the other rigid clusters. The second time scale, for particles in the largest rigid cluster, is obtained by examining motion relative to the second largest rigid cluster.

Figure 8 compares the moments of inertia for the fastest relaxation time in each pivot group, calculated by summing the exact moments of inertia of each cluster (I_{calc}) and (I_{est}) by summing moments of inertia given by $I=0.119s^{2.05}$. All the data are clustered close to the line given by $I_{\text{calc}}=I_{\text{est}}$, showing that the estimation is accurate.

We can now obtain time scales of relaxation for each pivot and free cluster using the appropriate moment of inertia. In Fig. 9 we have plotted the distribution of relaxation frequencies due to pivot and free clusters, for a number of bond densities. The analogous distributions of cluster sizes are provided in Ref. [30]. Close to the rigidity percolation transition, we see that the frequency distribution of unconstrained modes stretches continuously from the highest frequency to the lowest allowed by the system size. These results are in qualitative agreement with calculations for

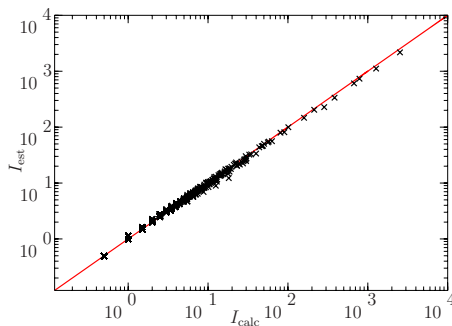


FIG. 8. (Color online) The total moment of inertia of a group of rigid clusters joined together by interdependent pivots is calculated by adding together the moments for the individual clusters, excluding the largest cluster. This is calculated by summing the exact moments of inertia of each cluster (I_{calc}) and by summing moments of inertia given by $I=0.119s^{2.05}$, where s is the size of the rigid cluster (I_{est}). The line shows $I_{\text{est}}=I_{\text{calc}}$.

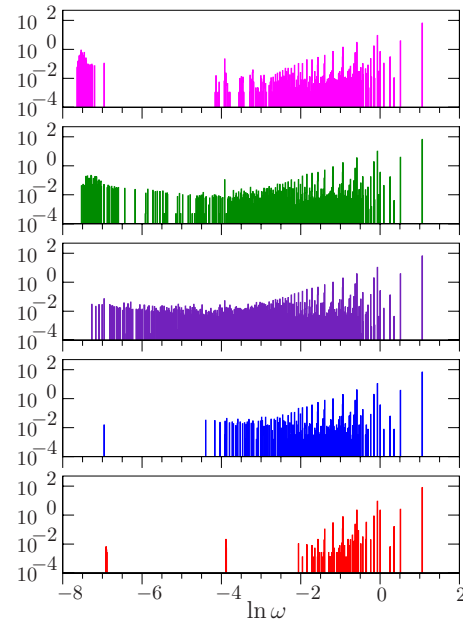


FIG. 9. (Color online) Normalized histograms showing average distributions of relaxation frequencies resulting from pivot and free clusters for five different bond densities—shown from bottom to top: 0.433, 0.597, 0.65, 0.66, and 0.67—on a double-logarithmic plot. Frequencies for both translational and rotational modes of free clusters are shown, as well as the two highest relaxational frequencies for each pivot cluster.

particles with short-range interactions [24]. For bond densities above the percolation transition, we see the distribution of frequencies break into two separate groups: one located around the high frequency while the other is centered at a frequency that vanishes with increasing system size. The appearance of this broad spectrum of soft modes is a characteristic of structures close to the rigidity percolation transition, i.e., structures of minimal rigidity. The reader is reminded that we have not included the phonon density of states, associated with a finite elastic constant for the bonds.

Examining the relaxational frequencies in Fig. 9, it is clear that some modes are limited only by the system size and are in fact of infinite extent. These modes should be excluded from our analysis and include the translation and rotation of the system as a whole. We find [30] that there is one large free cluster involving most of the system over nearly the whole range of bond densities. This free cluster is of infinite extent and we consider the motion of this cluster to have an infinite relaxation time as corresponding to motion of the system as a whole. However, particles within this cluster can still move through internal motion. A rigid cluster that spans the system should also be regarded as being of infinite extent and can be assigned an infinite relaxation time. Particles within a spanning rigid cluster cannot move. The largest free cluster is easily recognized but a spanning rigid cluster may or may not be present. We test for a spanning rigid cluster by replicating the system to form a 100×50 lattice. When the pebble game is rerun, a cluster is found to be spanning if the number of floppy modes is less than double the number in the original system. If the cluster spans in one direction, the number of modes is reduced by 2; if it

spans in both directions, the number of modes is reduced by 3. This method is very simple but can fail if the rigid cluster has few overconstraints and no longer exists as a single rigid cluster spanning the system when replicated. Such a cluster is only rigid due to the finite nature of the system. As the system size is increased, the extra degrees of freedom resulting from replication of the system can be absorbed more easily.

V. RELAXATION

In the model system we have described thus far, there are a fixed number of randomly applied constraints. We have omitted bond breakage and formation so that all bonds are treated as permanent. No particle contained within a rigid cluster that spans the system can relax, but *nonrigid* particles in the system can relax. In the following analysis, we will assume that such nonrigid particles can relax fully via their fastest relaxational mode. Note, however, that relaxation in a pivot cluster that spans the system is likely to be restricted. Strictly, even small free clusters may be unable to relax if sufficiently confined by their neighbors. The latter effect can be ignored as the number of free clusters left (in the random bond model, at least) at high bond density will be small.

We use the rotational relaxation expression due to Zwanzig [38] for the cog network to describe the structural relaxation of the permanent disordered network. In this expression, each individual particle relaxes as

$$\phi_i(t) = \exp(-\langle \Omega_i^2 \rangle t^2 / 2). \quad (3)$$

$\phi_i(t)=1$ for all the particles in spanning rigid clusters that cannot relax as we have effectively set their moments of inertia to ∞ . The overall relaxation is then

$$\Phi(t) = \frac{1}{N} \sum_{i=1}^N \phi_i(t). \quad (4)$$

When calculating the frequencies for each collective mode as plotted in Fig. 9, we found that some particles participated in many collective modes and hence could be associated with many different time scales. To calculate the relaxation function for each particle, we have chosen to simply assign to each particle the shortest relaxation time out of all the soft modes in which the particle participates.

Figure 10 shows $\Phi(t)$ for five different bond densities: 0.433, 0.597, 0.65, 0.66, and 0.67 averaged over 100 different bond configurations. For the two lowest densities, full relaxation occurs but relaxation is limited without bond changes for the higher densities. The cause of this lack of full relaxation is the existence of spanning rigid clusters as shown for single configurations in Fig. 11. This figure shows spatial maps of the relaxation time scales for each particle for the four higher bond densities. The darkest regions show the spanning rigid clusters where no relaxation can occur.

As bond density is increased toward the percolation transition, we see an increase in the size of different kinetic subregions as well as a growth in the distribution of time scales. Above the transition, the soft modes appear as increasingly isolated pockets embedded in a spanning rigid

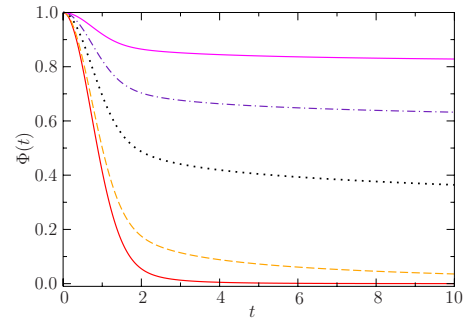


FIG. 10. (Color online) The overall relaxation $\Phi(t)$ averaged over 100 different random bond configurations for each of five different bond densities, shown from bottom to top: 0.433, 0.597, 0.65, 0.66, and 0.67. For the high bond densities, complete relaxation of the system does not occur for a fixed bond configuration; full relaxation would require changes in bond configuration.

cluster. This suggests that an inherent structure resembling a network close to the jamming transition will have a hyper-heterogeneous dynamics, while an inherent structure corresponding to a higher bond density will have dynamic heterogeneities reminiscent of point defects in solids.

Structural relaxation in a supercooled liquid requires that multiple inherent structures be visited. While we have postponed the inclusion of bond fluctuations to future work, we have examined the sensitivity of bond configurations at different densities when one bond is moved to a randomly chosen vacant position in the system. As shown in Fig. 12, this sensitivity also depends dramatically on the proximity of the system to the rigidity percolation point. Close to rigidity percolation, there is a high degree of sensitivity of the mode maps to changes in bond configuration. This sensitivity decreases rapidly as the bond density increases above the percolation value. Again, we are concerned with the shortest relaxation time for each site and examine the changes in these shortest relaxation times. We can quantify the changes in time scale by calculating the variance in time scale for each site for 100 different bond moves. This variance is given by

$$\sigma^2 = \langle (\tau_i - \langle \tau_i \rangle)^2 \rangle, \quad (5)$$

where τ_i is the shortest time scale for the site in the configuration formed by the i th bond move. For particles that cannot relax, in spanning clusters, we use a value of $\tau_i=1000$. Light gray areas, as shown by the top of the logarithmic scale bar, represent regions of no change. For intermediate bond densities, before and around the percolation transition, there are relatively large changes in time scale for most sites. At low and high densities, only small pockets of high variability are observed.

When we start to change a configuration by making single bond moves at these densities, we see that the general shape of the distribution of time scales does not change but that large changes in the spatial distribution of kinetics can be observed. If the spatial distribution of soft modes can be substantially changed by a small number of bond changes it would suggest (i) that the soft modes will be rapidly distributed through the system via bond fluctuations in stark con-

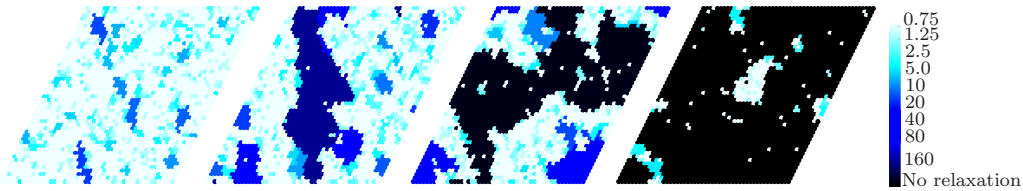


FIG. 11. (Color online) Spatial maps of the shortest relaxation time per particle for a number of different bond densities from left to right: 0.597, 0.65, 0.66, and 0.67. We consider each unconstrained motion in the system involving the translation or rotation of free clusters or the collective motion of groups of rigid clusters connected by interdependent pivots. Each site on the lattice may be involved in any number of unconstrained motions but is assigned a time scale according to the mode with the maximum thermal velocity. The logarithmic scale gives the relaxation time for each site.

trast to diffusing defect models and (ii) that the spatial distribution of soft modes can provide little information about the long-time evolution of the configuration. The changing spatial distribution is also relevant when using dynamic heterogeneities to identify a dependence on the underlying structure. This method requires a connection to exist between structure and the spatial pattern of the dynamics. Specifically, if small variations in structure can produce huge changes in the pattern of the dynamics, then the analysis of the dynamics will need to be quite sophisticated.

However, although we see that the spatial distribution of modes can change dramatically as a result of small changes in configuration, these changes are directly related to the underlying structure via changes in the arrangement of rigidity within the system. It is possible to equate the changes in relaxation times shown by the maps with changes in the size of rigid clusters. Determination of relaxation times for the original configuration required the knowledge of motions in the form of interdependent pivots and isolated or free clusters, both of which can be composed of many rigid clusters. For the pivot groups, the total moment of inertia and hence the relaxation time are found by summing the moments of inertia of constituent rigid clusters. If moving one bond results in a change in size of one of the rigid clusters, this change in size gives the change in the total moment of inertia via the relation $I=0.119s^{2.05}$; hence, $\Delta\sqrt{I}\approx 0.345\Delta s$. For free clusters, relaxation is given by the sum of the masses of constituent rigid clusters and hence any change in the size of a constituent rigid cluster can again be directly related to a change in relaxation time.

The two panels in Fig. 13 compare changes in relaxation time scale with changes in the size of rigid clusters. The left panel shows the distribution of changes in fastest relaxation time scales for 100 single bond moves from the same initial configurations for four different bond densities (as shown in Fig. 11). The right panel shows the changes in rigid cluster

size for the same bond moves. The change in rigid cluster size has been scaled by 0.345 to allow a direct comparison between the two panels. It is clear that changes in the rigid cluster sizes are directly responsible for the time scale changes. However, although this gives a structural cause to the evolving heterogeneity, the nontrivial aspect of this connection is relating changes in rigid cluster size in one part of the system to the resulting time scale changes, which can occur throughout the system.

VI. DISCUSSION

In a paper on the gel transition in 1991, Martin *et al.* [39,40] began their discussion of the theory of relaxation as follows: “at this point it is probably evident to the perspicacious reader that the phenomenology of the relaxation of density fluctuations in gels is complex (or at least not simple).” The challenge of describing relaxations which are “at least not simple” not only persists, but has, over the ensuing 17 years, become increasingly identified as the common essential element for progress in understanding a broad range of materials: glass-forming liquids, proteins, colloidal suspensions, microemulsions, and granular materials.

In a cluster description of complex relaxation, attention is focused on the small displacements associated with the relaxation of structure and stress. Coupling of the motion of different clusters is neglected. For the gel transition [39,40], such a coupling has been described in terms of a cluster of size R diffusing in a medium whose viscosity has contributions from the clusters of size less than R and whose confinement is determined by clusters of size greater than R .

Collective motion is explicitly considered for relaxation in our constraint network. A partial treatment of collective motion and its cooperative character emerges through pivot connections between rigid clusters. Constraints induce local rigidity forcing a group of particles to move as one while

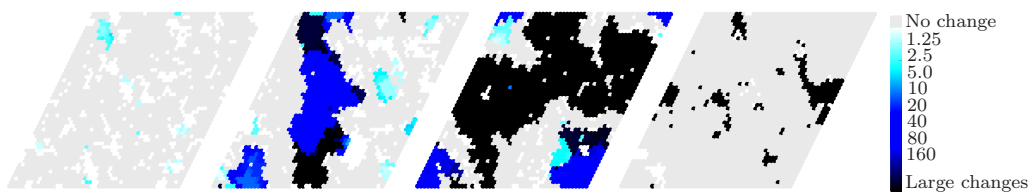


FIG. 12. (Color online) Spatial maps of the variance in shortest relaxation time for each particle at a number of different bond densities from left to right: 0.597, 0.65, 0.66, and 0.67. The variance is given by comparing time scales for 100 systems formed by one bond change from the same initial configuration as shown in Fig.11. The logarithmic scale gives the variance in relaxation time for each site.

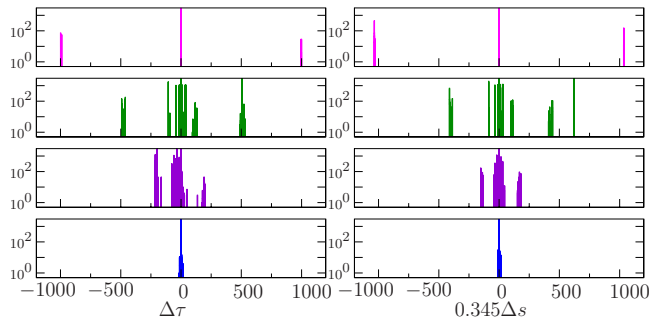


FIG. 13. (Color online) The two panels show changes recorded for 100 single bond moves from initial configurations at four different densities, from bottom to top: 0.597, 0.65, 0.66, and 0.67. The left panel shows the distribution of changes in the shortest relaxation time scale for each site ($\Delta\tau$) and the right panel shows the changes in rigid cluster size (Δs) for the same bond moves. The change in rigid cluster size has been scaled by 0.345 to allow a direct comparison between the two panels.

pivots link these clusters so that motion of one can only occur with the cooperative motion of the other clusters in the pivot group. However, our pattern of constraints does not change with motion. The rotation of a rigid cluster through any finite angle could result in new interactions with clusters not initially connected via any constraints. For the nonlinear response of the network, such a *geometrical* confinement is of considerable importance. However, we suggest that it is the *topological* character of the constraints, treated here, that dominates the linear response.

Two important features of the constraints have not been dealt with in this paper. While we have not considered bond relaxation in this paper, it is clear that the kinetics of bond breaking and making may well be related to the kinetics of the unconstrained motions remaining in the network. This is an acknowledgment that the lifetime of each bond is determined, not just by the stability of the isolated bond, but also that of the extended network in which it resides. In a recent simulation study of the viscosity in molten mixtures of LiF and the network-forming BeF_2 , Salanne *et al.* [41] noted just such an increase in the lifetime of BeF bonds with the concentration of BeF_2 , an increase that matched that observed for the viscosity.

Our second omission concerns the link between our configurations, representing inherent structures, and the sampling of these structures in a trajectory at finite temperature. A proper treatment of this will involve both the inclusion of the energy associated with bonds and any interactions, attractive or repulsive, between bonds and a specific description of the kinetics associated with fluctuations in the bond network. With bond density as the control parameter, the path from simple liquid to disordered solid via a rigidity percolation transition is straightforward and inevitable. There are, however, a number of possibilities for the liquid to solid transition when temperature is the control parameter. Work addressing both these limitations of the present study is currently underway.

The structures considered in this paper are formed by randomly placing bonds within a 2D triangular lattice. Different protocols for building the network can be considered, such as stress avoidance (disallowing redundant bonds) or bond aggregation (favoring overconstrained regions). Systems formed using these different protocols also show rigidity percolation and total rigidity transitions. A larger space of possible inherent structures can be considered by combining different protocols and this may be relevant for examining the behavior of different glass-forming systems.

VII. CONCLUSION

In this work, we have shown how one can obtain a unique spatial resolution of the motions that remain unconstrained, starting with a generic description of a disordered solid. The character of this distribution is found to change significantly, depending on whether the solid is close to a rigidity percolation or to the onset of total rigidity itself where all unconstrained motions vanish. Alongside this dramatic change in spatial distribution, we find substantial changes in the manner in which these heterogeneities are expected to evolve in time. While for solids near rigidity the isolated unconstrained motions will evolve incrementally, near the rigidity percolation, the changes are expected to be abrupt and extend over large regions of the sample.

Local mode structure can provide powerful insights into complex cooperative dynamics [3,22]. This study was motivated by a desire to provide a model of the local minima, or inherent structures, of a supercooled liquid using a description of amorphous rigidity. We have not addressed, nor was it our goal to do so, the question of where the inherent structures of a particular supercooled liquid should lie along our spectrum of rigid disordered networks, ranging from rigidity percolation to total rigidity. The dynamic heterogeneity of the soft modes varies considerably over this spectrum. We find that both the degree of heterogeneity of the local mode structure and its sensitivity to small configuration changes exhibit clear maxima on approaching the rigidity percolation from either direction in bond density. Such behavior is reminiscent of the avalanches described in particle simulations [10]. In contrast, inherent structures that are better described by higher bond densities would be characterized by isolated soft modes embedded in the spanning rigid cluster. The gradual evolution of these highly localized soft modes with configurational change would resemble something more like defect diffusion.

ACKNOWLEDGMENTS

We would like to acknowledge helpful conversations with Paul Madden, Ken Schweizer, and Michael Thorpe as well as the valuable assistance provided by the website maintained by Michael Thorpe in implementing the Pebble Game algorithm. This work was supported by the Australian Research Council through its Discovery Program.

- [1] K. Binder and W. Kob, *Glassy Materials and Disordered Solids: An Introduction to Their Statistical Mechanics* (World Scientific, Singapore, 2005).
- [2] N. Xu, M. Wyart, A. J. Liu, and S. R. Nagel, Phys. Rev. Lett. **98**, 175502 (2007).
- [3] A. Widmer-Cooper, H. Perry, P. Harrowell, and D. R. Reichman, Nat. Phys. **4**, 711 (2008).
- [4] M. Goldstein, J. Chem. Phys. **51**, 3728 (1969).
- [5] F. H. Stillinger and T. A. Weber, Phys. Rev. A **25**, 978 (1982).
- [6] D. J. Wales, *Energy Landscapes* (Cambridge University Press, Cambridge, England, 2003).
- [7] D. J. Wales, Philos. Trans. R. Soc. London, Ser. A **363**, 357 (2005).
- [8] A. Heuer, J. Phys.: Condens. Matter **20**, 373101 (2008).
- [9] F. Sciortino, J. Stat. Mech.: Theory Exp. **2005**, P05015.
- [10] C. Brito and M. Wyart, J. Stat. Mech.: Theory Exp. **2007**, L08003.
- [11] J. C. Phillips, J. Non-Cryst. Solids **34**, 153 (1979).
- [12] M. F. Thorpe, J. Non-Cryst. Solids **57**, 355 (1983).
- [13] J. C. Maxwell, Philos. Mag. **27**, 294 (1864).
- [14] D. J. Jacobs and M. F. Thorpe, Phys. Rev. Lett. **75**, 4051 (1995).
- [15] D. J. Jacobs and M. F. Thorpe, Phys. Rev. E **53**, 3682 (1996).
- [16] A. J. Liu and S. R. Nagel, Nature (London) **396**, 21 (1998).
- [17] E. Guyon, S. Roux, A. Hansen, D. Bideau, J. P. Troadec, and H. Crapo, Rep. Prog. Phys. **53**, 373 (1990).
- [18] A. S. Clarke and H. Jonsson, Phys. Rev. E **47**, 3975 (1993).
- [19] C. F. Moukarzel, Phys. Rev. Lett. **81**, 1634 (1998).
- [20] A. Donev, S. Torquato, and F. H. Stillinger, Phys. Rev. E **71**, 011105 (2005).
- [21] W. Ellenbroek, Z. Zeravcic, W. van Sarrloos, and M. van Hecke, EPL **87**, 34004 (2009).
- [22] D. J. Jacobs, A. J. Rader, L. A. Kuhn, and M. F. Thorpe, Proteins: Struct., Funct., Genet. **44**, 150 (2001).
- [23] M. F. Thorpe, <http://flexweb.asu.edu>, 2008.
- [24] L. E. Silbert, A. J. Liu, and S. R. Nagel, Phys. Rev. Lett. **95**, 098301 (2005).
- [25] M. Wyart, S. R. Nagel, and T. A. Witten, EPL **72**, 486 (2005).
- [26] M. Wyart, H. Liang, A. Kabla, and L. Mahadevan, Phys. Rev. Lett. **101**, 215501 (2008).
- [27] C. S. O'Hern, L. E. Silbert, A. J. Liu, and S. R. Nagel, Phys. Rev. E **68**, 011306 (2003).
- [28] G. Biroli, Nat. Phys. **3**, 222 (2007).
- [29] O. Dauchot, G. Marty, and G. Biroli, Phys. Rev. Lett. **95**, 265701 (2005).
- [30] V. K. de Souza and P. Harrowell, Proc. Natl. Acad. Sci. U.S.A. **106**, 15136(2009).
- [31] C. P. Moukarzel, in *Rigidity Theory and Applications*, edited by M. F. Thorpe and P. M. Duxbury (Kluwer Academic/Plenum Publishers, New York, 1999), p. 125.
- [32] R. Connelly, in *Rigidity Theory and Applications*, edited by M. F. Thorpe and P. M. Duxbury (Kluwer Academic/Plenum Publishers, New York, 1999), p. 47.
- [33] R. Connelly, K. Rybnikov, and S. Volkov, J. Stat. Phys. **105**, 143 (2001).
- [34] M. Micoulaut and J. C. Phillips, J. Non-Cryst. Solids **353**, 1732 (2007).
- [35] C. C. Jolley, S. A. Wells, B. M. Hespeneheide, M. F. Thorpe, and P. Fromme, J. Am. Chem. Soc. **128**, 8803 (2006).
- [36] H. Gohlke and M. F. Thorpe, Biophys. J. **91**, 2115 (2006).
- [37] D. J. Jacobs and M. F. Thorpe (unpublished).
- [38] R. Zwanzig, J. Chem. Phys. **87**, 4870 (1987).
- [39] J. E. Martin, D. Adolf, and J. P. Wilcoxon, Phys. Rev. Lett. **61**, 2620 (1988).
- [40] J. E. Martin, J. Wilcoxon, and J. Odinek, Phys. Rev. A **43**, 858 (1991).
- [41] M. Salanne, C. Simon, P. Turq, and P. A. Madden, J. Phys. Chem. B **111**, 4678 (2007).